Quantum Electronics **35** (5) 407 – 414 (2005)

NONLINEAR OPTICAL PHENOMENA

PACS numbers: 42.65.Re; 42.70.Nq; 72.40.+w
DOI: 10.1070/QE2005v035n05ABEH002805

Competition between linear and nonlinear processes during generation of pulsed terahertz radiation in a ZnTe crystal

V.Ya. Gaivoronskii, M.M. Nazarov, D.A. Sapozhnikov,
E.V. Shepelyavyi, S.A. Shkel'nyuk, A.P. Shkurinov, A.V. Shuvaev

***Abstract*. The generation of terahertz (THz) pulses by the optical rectification of femtosecond laser pulses in a ZnTe crystal is studied. A substantial decrease in the THz radiation power was observed upon tight focusing of laser radiation into the crystal. It is shown that the consideration of competing two-photon absorption and second-harmonic generation processes proceeding simultaneously with optical rectification cannot explain this effect even qualitatively. It is assumed that the observed decrease in the THz radiation power is caused by a decrease in the size of a source of nonlinear polarisation. The conditions are found for the most efficient generation of THz radiation in the ZnTe crystal.**

Keywords: *optical rectification, terahertz pulsed radiation, nonlinear-optical crystals.*

1. Introduction

Terahertz frequencies ($10^{11} - 10^{13}$ Hz) are located in the presently inaccessible far-IR spectral range corresponding to submillimetre wavelengths [1, 2]. This spectral range is of great interest for spectroscopy because the vibrational frequencies of molecules in gases and liquids, optical phonon frequencies in solids, vibrational frequencies of polyatomic biological molecules, etc. lie in this range. Terahertz spectroscopy and microscopy is widely used in biology, medicine [3], and semiconductor physics. Along with continuous submillimetre radiation from lasers and lamp sources, terahertz (THz) pulses [4] generated by femtosecond laser pulses of the optical range are widely employed in the last years. The THz pulse duration is 1 – 1.5 cycles of the electromagnetic field, corresponding to the Fourier spectrum extending from zero to a few terahertz. Note that the spectral width (FWHM) of the THz pulse is comparable to its central frequency equal to ~ 0.7 THz or exceeds it.

S.A. Shkel'nyuk, A.P. Shkurinov, A.V. Shuvaev Department of Physics, M.V. Lomonosov Moscow State University, Vorob'evy gory, 119992 Moscow, Russia; e-mail: alex@lasmed.phys.msu.su;
M.M. Nazarov, D.A. Sapozhnikov International Teaching and Research Laser Center, M.V. Lomonosov Moscow State University, Vorob'evy gory, 119992 Moscow, Russia; e-mail: maxim@lasmed.phys.msu.su;
V.Ya. Gaivoronskii, E.V. Shepelyavyi Institute of Physics, National Academy of Sciences of Ukraine, prosp. Nauki 46, 03028 Kiev, Ukraine

Received 30 April 2004; revision received 19 November 2004
Kvantovaya Elektronika **35** (5) 407 – 414 (2005)
Translated by M.N. Sapozhnikov

There exist several techniques for generating THz pulses [1, 2, 4]. The THz pulses were first generated with the help of dipole antennas based on the Auston switch [5, 6], in which pulsed radiation is generated due to nonstationary electron – hole photoconductivity of a semiconductor induced by short light pulses [7]. The THz pulse detection with a photoconductive dipole antenna is based on the same principle [5 – 7]. A specific feature of the THz pulse detection with the help of an antenna [5] or a nonlinear crystal [8] is the possibility of direct measuring the strength and direction of the THz pulse electromagnetic field, thereby obtaining information on the pulse amplitude and phase and calculating then the refractive index and absorption coefficient of a medium under study [2].

In media with the second-order nonlinear susceptibility $\chi^{(2)}$, THz pulses can be produced by generating the difference frequency; and in the frequency-degenerate case – by optical rectification [8 – 10], when an optical pulse with a broad spectral width $\Delta\omega$ at the frequency $\Omega \approx \omega_2 - \omega_1 \approx \Delta\omega \ll \omega_{\rm opt}$ induces polarisation

$$P_i^{(2)}(\Omega) = \chi_{ijk}^{(2)}\left(\Omega; \omega + \frac{\Delta\omega}{2}, -\omega + \frac{\Delta\omega}{2}\right) \times E_j\left(\omega + \frac{\Delta\omega}{2}\right) E_k\left(\omega - \frac{\Delta\omega}{2}\right) \quad (1)$$

in the medium. For example, for a 60-fs laser pulse of spectral width $\Delta\lambda \approx 15 - 30$ nm, the difference frequency Ω lies in the range from a few fractions to tens of terahertz. The THz pulse generation efficiency is determined in this case by the phase-matching parameters, the nonlinear susceptibility and length of the crystal and is $\sim 10^{-6}$ [2, 11, 12].

This paper is devoted to the study and optimisation of the THz pulse generation in a $\langle 110 \rangle$ oriented ZnTe crystal, which is considered now as one of the most efficient materials for generating THz pulses upon excitation by a 800-nm Ti : sapphire laser. Unlike other crystals with a higher nonlinear susceptibility, the ZnTe crystal is virtually transparent in the frequency region 0.1 – 3 THz and phase-matching conditions for the THz pulse generation are well fulfilled in it [13]: $n_{\rm gr} = n_{\rm ter}$, where $n_{\rm gr} = n_{\rm ph} - \lambda({\rm d}n_{\rm ph}/{\rm d}\lambda)$; $n_{\rm ter} \approx \varepsilon_0^{1/2}$; ε_0 is the static dielectric susceptibility; $n_{\rm gr}$ and $n_{\rm ph}$ are the refractive indices for the group and phase velocities of the optical pulse, respectively; and $n_{\rm ter}$ is the refractive index in the THz range. The linear and nonlinear properties of ZnTe also attract interest because this crystal, being a good electro-optic material, can be used not only for generating but also for electro-optic recording THz pulses [13].

When a ZnTe crystal is irradiated by a high-power laser pulse, apart from optical rectification, competing nonlinear-optical processes such as second-harmonic generation (SHG) and two-photon absorption (TPA) occur [14]. In this paper, we observed a considerable decrease in the THz pulse power upon tight focusing of optical radiation into a nonlinear-optical crystal and discuss the mechanisms that can be responsible for this effect. By using the open-aperture z-scan method, we estimated the TPA coefficient and showed that TPA and SHG do not play any substantial role in the decrease of the THz pulse generation efficiency for the laser intensity used in experiments. We also investigated the dependences of the THz pulse generation efficiency on the power, intensity, and diameter of a focused laser beam.

2. Experimental

The scheme of the experimental setup is shown in Fig. 1a. A source of optical radiation was a femtosecond Ti : sapphire laser emitting 100-fs, 1-nJ pulses with a pulse repetition rate of 100 MHz. The laser pulses tunable in the range from 730 to 830 nm had a spectral width of 12 nm. The laser radiation was focused to a ZnTe crystal, where 2-ps THz pulses (Fig. 1b) of the spectral width up to 2.5 THz (Fig. 2) were generated. By neglecting dispersion in the nonlinear crystal, the temporal profile of the THz pulse should have the form of the second derivative of the optical pulse envelope [2].

The THz radiation was detected with a dipole photoconductive antenna [7]. The probe laser pulse was focused on the antenna in the space between two conductors deposited on a gallium arsenide substrate. The THz pulse being measured was focused with a silicon lens to the space between conductors from the other side of the antenna (Fig. 1a). We measured the dependence of the current produced in the antenna on the time delay Δt between the THz and probe optical pulses. Below, the maximum value of the THz pulse temporal profile (Fig. 1b) was treated as the amplitude of the THz pulse field. The complex spectrum of the THz pulse, containing information on refraction and absorption in the medium through which the THz pulse has propagated, is calculated from the temporal THz pulse profile $E_{ter}(\Delta t)$ using the Fourier transform [15]. The experimental setup had a time resolution of 100 fs and a spectral resolution of 0.008 THz. A liquid helium-cooled QSiB/2 bolometer (QMC Instruments Ltd.) was used to measure the integrated (over the spectrum) THz pulse power.

Laser radiation incident on the THz pulse generator was modulated at the frequency 1 kHz, and the antenna (or bolometer) current was detected with a lock-in SR-810 amplifier (Stanford Research Systems) at the modulation frequency. A signal averaged for 300 ms was measured.

A ZnTe crystal with the $\langle 110 \rangle$ orientation had the form of a plane–parallel plate. We used two square samples of thickness $d = 2$ and 0.28 mm with a side of 1 cm. The band gap of ZnTe is 2.26 eV [16], the electro-optic coefficient is $r_{14} = 4 \times 10^{-12}$ m V^{-1} [17], and the carrier concentration is typically $\sim 10^{16}$ cm^{-3}. The measured optical parameters of the ZnTe crystal used in our experiments are presented in Table 1, where the typical optical characteristics of the crystal taken from [1, 13, 17–20] are also listed. Figure 2 shows the typical spectra of absorption, two-photon luminescence, SHG, THz pulse, and laser radiation at the fundamental frequency ($h\nu = 1.614$ eV, $\lambda = 770$ nm).

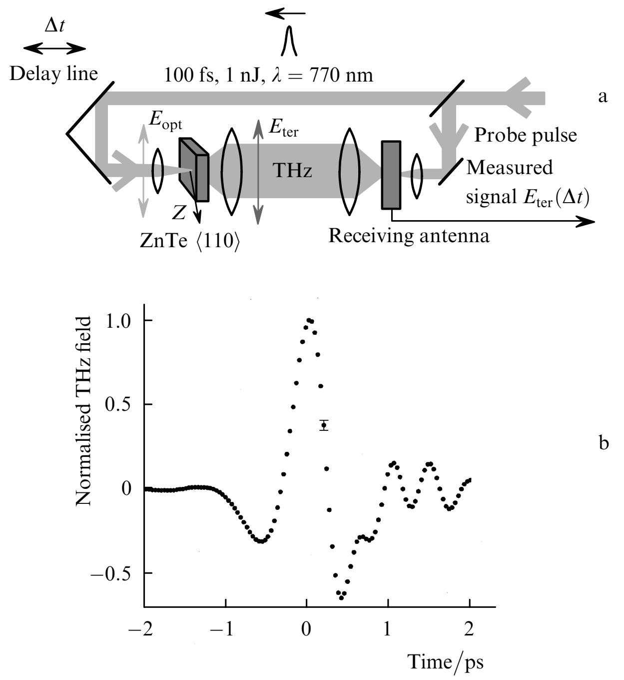

Figure 1. Scheme of the THz pulse generation and detection with a dipole antenna (Z is the crystallographic axis direction; the double arrows show the direction of polarisation of the optical and terahertz fields; the THz beams are collimated and focused by parabolic mirrors) (a) and the measured temporal profile of the THz pulse field (the THz pulse generator is a 2-mm thick ZnTe crystal, the laser wavelength is 770 nm) (b).

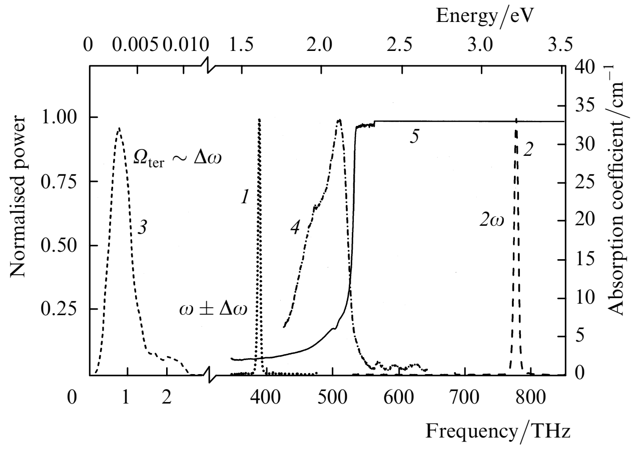

Figure 2. Fundamental radiation (*1*), second harmonic (*2*), optical rectification (*3*), and two-photon luminescence (*4*) spectra observed for the ZnTe crystal excited at 770 nm, and the absorption spectrum of ZnTe (*5*).

Because of a high refractive index of ZnTe ($n = 2.8-3.2$), reflection from each of the crystal faces is $\sim 30\,\%$ both for optical and THz frequencies, which reduces the conversion efficiency of optical radiation to THz pulses by $60\,\%$. Note that reflection losses can be substantially reduced by applying antireflection coatings for laser radiation to the front face of the crystal and for THz

Table 1. Parameters of the 2-mm thick ZnTe crystal in the optical and terahertz regions.

Data	Optical range ($\lambda = 770$ nm)							
	n_{ph}	n_{gr}	α/cm^{-1}	$\beta/\text{cm GW}^{-1}$	R_{tot}	T_{tot}	θ/deg	θ_B/deg
Experimental	2.8 ± 0.1	3.27 ± 0.1	2 ± 0.5	20 ± 5	0.37 ± 0.03	0.58 ± 0.05	20	71
Reference	2.87	3.36	8; 3	4.7				
	Terahertz range ($\lambda = 1$ mm – 120 μm, $\Omega = 0.3 - 2.5$ THz)							
	n_{ter}	α/cm^{-1}	R_{tot}	T_{tot}	θ/deg	θ_B/deg		
Experimental	3.18 ± 0.05	1 – 5	0.35 ± 0.03	0.55 ± 0.05	18	73		
Reference	3.17	1 – 3						

Notes: α is the linear absorption coefficient; β is the nonlinear absorption coefficient; R_{tot} is the ratio of the reflected average THz field to the average incident field (averaging was performed over the time interval much longer than the reflection period); T_{tot} is the ratio of the total transmitted THz field to the average incident field; θ is the total internal reflection angle; θ_B is the Brewster angle.

radiation [21] to the rear face of the crystal or by cutting the crystal at the Brewster angle (72°) to the $\langle 110 \rangle$ axis.

The maximum THz pulse generation efficiency was observed for the normal incidence of the laser beam on a sample, when the angle between the Z axis of the crystal and polarisation direction of laser radiation was 54°. In this case, the direction of THz pulse polarisation coincided with that of laser radiation (Fig. 1a).

The data on refraction and absorption in the THz frequency region were obtained by processing the complex spectra of the THz pulse incident on the crystal and transmitted through it. By measuring the THz pulse delay after propagation through the crystal, we can also measure the refractive index averaged over the entire THz pulse spectrum. Due to a weak dispersion of the ZnTe crystal, there is no substantial difference between the group and phase refractive indices in this frequency region.

The efficiency of nonlinear optical absorption was estimated by the open-aperture z-scan method [22]. The laser beam was focused by lens 1 into a sample (Fig. 3). The light wave intensity in the sample depended on the distance z between the sample and lens and the focal distance f of the lens (the distance between the focal point and the beam waist position for lenses with $f = 50$, 70, 80, and 180 mm used in experiments was small, and we neglected it). The laser beam radius r_0 (at which the field amplitude decreases by a factor of e) on the focusing lens 1 was 1 mm and the beam waist radius decreased down to $r_{min} = 12$ μm for $f = 50$ mm. When a sample was displaced along the optical axis z, the intensity of laser radiation on the sample changed (increasing with decreasing $|z - f|$). The dependence of the transmission coefficient of the sample on $|z - f|$ was measured in experiments.

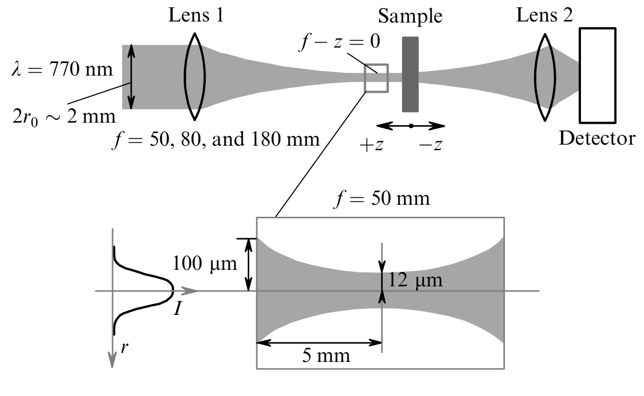

Figure 3. Scheme illustrating the z-scan method.

By using the z-scan method, we assumed that the measurement of the THz pulse generation efficiency as a function of the laser beam focusing (the value of $|z - f|$) will give information about its dependence on the laser beam diameter and intensity. Unlike the optical z-scan method, in the case of THz z-scan the positions of a crystal under study and THz pulse detector were not changed, whereas the distance between the crystal and lens focusing optical radiation was varied and the amplitude (or power detected by a bolometer) of generated THz pulses was measured.

3. Discussion of the results

Because the optical rectification efficiency (the power ratio P_{ter}/P_{opt} for THz and light pulses) linearly depends on the intensity of radiation incident on a sample, at first glance the simplest method to increase the THz pulse power is to focus laser radiation more tightly into a nonlinear crystal, thereby increasing the intensity of radiation incident on the THz generator. However, this is not confirmed experimentally upon tight focusing, when the laser beam diameter becomes comparable with the THz radiation wavelength.

Figure 4 shows the experimental dependence of the THz pulse power on the crystal position with respect to the laser beam waist. This dependence demonstrates the unexpected result at first glance: the THz pulse generation efficiency considerably decreases in the case of a very tight radiation focusing into a ZnTe crystal. A deep minimum – 'the z-hole' observed at $z - f = 0$ corresponds to the maximum intensity

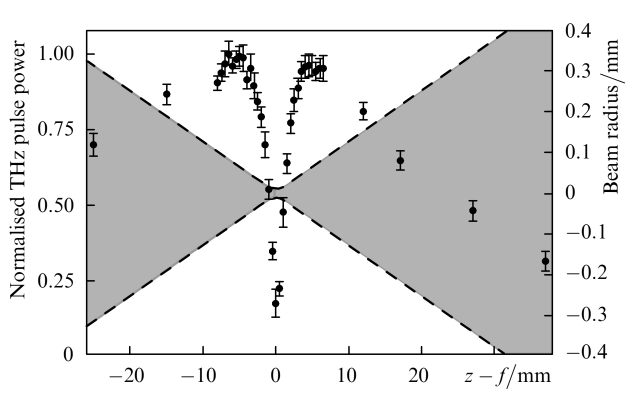

Figure 4. Dependences of the THz radiation power measured with a bolometer (points) and the beam radius (dashed straight lines) on the distance $z - f$ between the crystal centre and the lens focus for the crystal thickness $d = 2$ mm, the focal distance $f = 80$ mm (the waist length is $l_d \sim 1$ mm), and the average laser radiation power 170 mW.

of laser radiation in the ZnTe crystal. The z-hole width $|z-f|$ is comparable with the waist length l_d of a focused laser beam: $|z-f| \leqslant l_d = ka^2/2 \sim 1$ mm, where k is the wave number and a is the transverse size of the beam waist. To explain this effect, we investigated in detail the optical characteristics of the ZnTe crystal used for generating THz pulses.

A ZnTe crystal is a semiconductor [16] which is virtually transparent in the emission region of the laser used in experiments. We determined the fundamental absorption edge $E_g = 2.26$ eV ($\lambda = 550$ nm) with the help of the Urbach rule. When the crystal is irradiated by the intense light, green – yellow non-directional luminescence caused by TPA is visually observed on the crystal surface and directional SHG radiation strongly absorbed in the crystal volume.

3.1 Influence of TPA on the THz pulse generation efficiency

We analysed qualitatively the experimental data by using the model of nonlinear absorption of light at the fundamental frequency. We assumed that radiation was attenuated due to TPA and SHG in the ZnTe crystal. The equation describing the nonlinear absorption of light in a sample has the form

$$\frac{dI}{dz} = -\alpha I - \beta I^2, \tag{2}$$

where α is the linear absorption coefficient and β is the nonlinear absorption coefficient. The contribution of cascade absorption, which is described by the cubic term, was neglected in (2).

The contributions of TPA and SHG to the attenuation of incident laser radiation can be divided by using polarisation dependences because the TPA and SHG efficiencies are determined by tensors of different ranks. For maximum TPA ($z-f=0, f=50$ mm), the azimuthal angle φ between the crystal axis Z and the direction of laser radiation polarisation was changed from 0 to $\pi/2$. In this case, the SHG intensity changed by two orders of magnitude, whereas the transmission of fundamental radiation changed only by 6 %. Therefore, the influence of SHG on the attenuation of transmitted radiation is insignificant. Upon intense optical excitation of semiconductors, free carriers can be generated, which should substantially enhance the absorption of THz pulses [23]. However, this does not play a significant role under our experimental conditions. We assume below that the nonlinear absorption coefficient β is a scalar quantity and is determined only by TPA.

The intensity of focused radiation incident on the crystal was calculated in the parabolic approximation of the diffraction theory for Gaussian beams [24] for a thin ($d = 0.28$ mm) sample. The transmission coefficient for a pulse with Gaussian distributions over time and the transverse coordinate can be obtained from (2) in the form

$$T = \frac{e^{-\alpha z}}{\sqrt{\pi} q} \int_{-\infty}^{\infty} \frac{\ln\left(q e^{-t'^2} + 1\right)}{e^{-t'^2}} dt', \tag{3}$$

where $q = I_0 L_{eff} \beta$; $t' = t/\tau$ is the pulse duration; $L_{eff} = (1 - e^{-\alpha d})/\alpha$ is the effective crystal length; $I_0(z) = W_p \times [\pi^{3/2} \tau r^2(z)]^{-1}$ is the peak intensity on the beam axis, which is determined by the mutual arrangement of the lens and sample; $r^2(z) = r_0^2[(1-z/f)^2 + (z/l_d)^2]$; $r_0 = 1$ is the beam radius in front of the lens; and W_p is the pulse energy. The consideration of the pulse duration in the model leads to an increase in the calculated value of β by several times.

The z-scan method is based on analysis of the dependence of the transmission coefficient T on the lens coordinate z at the constant power P_{opt}. Figure 5a shows the dependences of the transmission coefficient on the distance between the crystal and lens focus for $P_{opt} \propto W_p = $ const, and Fig. 5b presents the dependences of the intensity of transmitted radiation on the incident radiation intensity for $z = $ const. By comparing the model and experimental dependences (Fig. 5a), we can calculate the parameter β.

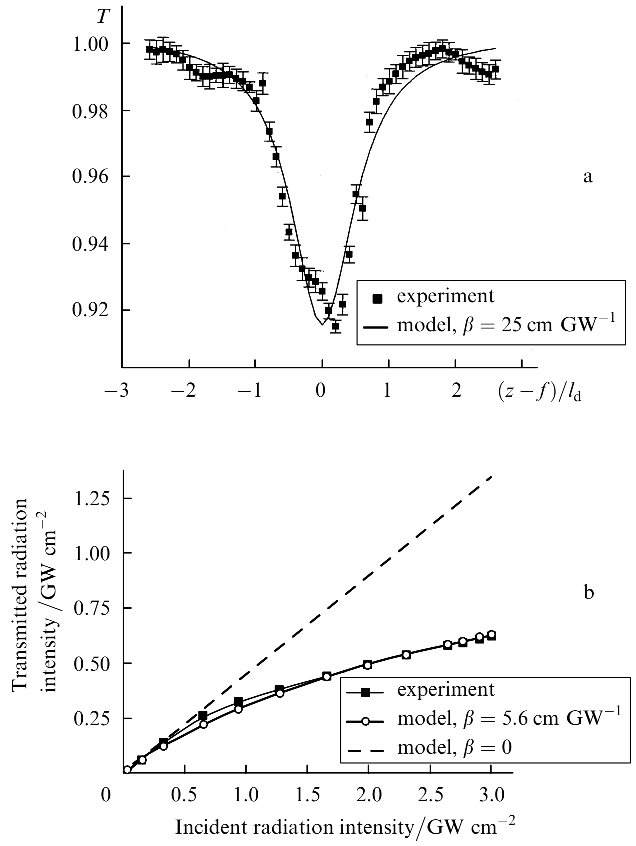

Figure 5. Dependences of the transmission coefficient T of the ZnTe crystal on the normalised distance $(z-f)/l_d$ ($f = 80$ mm, $l_d = 4.7$ mm, $\lambda = 770$ nm) for a thin sample with $d = 0.28$ mm $\ll l_d$ (a) and the dependences of the laser radiation intensity transmitted through the crystal located in the beam waist on the incident radiation intensity ($f = 70$ mm, $l_d = 1$ mm, $z - f = 0$) for a thick sample with $d = 1$ mm $> l_d$ (b).

The influence of the laser intensity on nonlinear absorption is demonstrated in Fig. 5b. The difference from a linear dependence is noticeable only for a thick sample. Because a thick sample ($d = 2$ mm $> l_d$) does not satisfy the requirements of the TPA model and the cascade absorption of laser radiation was neglected, the model curve agrees with the experimental curve only for $\beta = 5.6$ cm GW^{-1}, which is smaller by a factor of four than the correct value 20 cm GW^{-1}.

The spatial distribution of the Ti : sapphire laser beam intensity slightly differs from a Gaussian profile, which introduces the error of no more than 30 % to the measurement of the absolute values of β. The nonlinear absorption coefficient β for our crystals calculated in these approximations was 20 ± 5 cm GW^{-1}.

Consider the dependence of the THz pulse power P_{ter} on the distance z between a lens and a crystal taking into account linear and two-photon absorption. The expression for the THz pulse power in the case of only linear absorption has the form

$$P_{\mathrm{ter}} \propto d_{14}^2 \frac{1 - \mathrm{e}^{-2\alpha d}}{2\alpha\pi^2} \left[\frac{W_{\mathrm{p}}}{\tau r(z)} \right]^2,$$

where $d_{14} \propto \chi^{(2)}$ is the nonlinear-optical susceptibility. The dependence $P_{\mathrm{ter}}(z)$ can be obtained analytically, taking into account linear and nonlinear absorption, only in the case of cw laser radiation (for pulsed radiation, the correction coefficient for P_{ter} should be taken into account):

$$P_{\mathrm{ter}} \propto P_{\mathrm{opt}}^2 \left\{ \left[\frac{I_0(z)\beta + \alpha}{\beta^2} \right] \left[1 - \frac{1}{1 + I_0(z)\beta L_{\mathrm{eff}}} \right] + \frac{\alpha}{\beta^2} \ln \left[\frac{1}{1 + I_0(z)\beta L_{\mathrm{eff}}} \right] \right\} \pi r^2(z). \quad (4)$$

Figure 6a shows the dependences of the THz pulse power on the longitudinal coordinate z calculated from (4), including the case $\beta = 0$, when nonlinear absorption is absent. Near the laser beam waist ($|z - f| < l_{\mathrm{d}}$), the

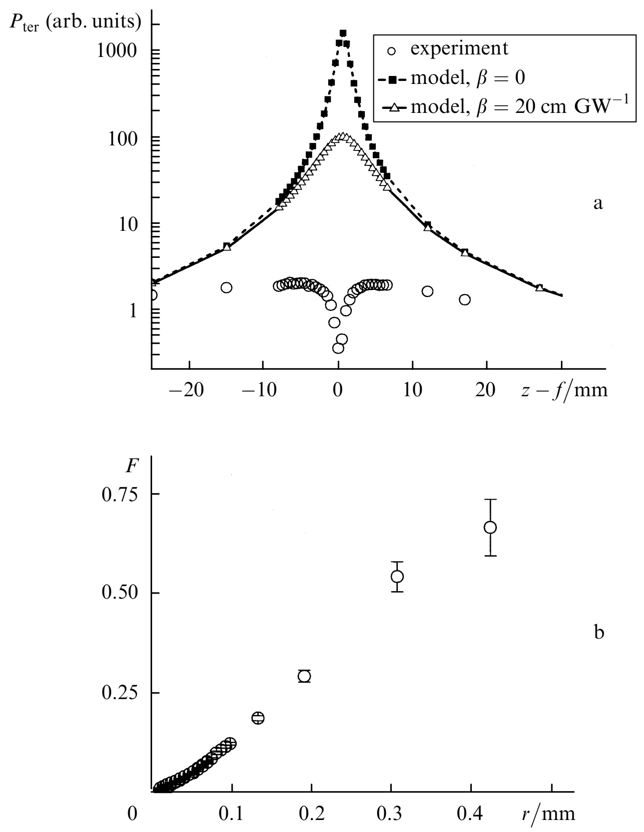

Figure 6. Model and experimental dependences of the THz pulse power on the distance $z - f$ taking into account linear and two-photon absorption for $d = 2$ mm (experimental points correspond to the data presented in Fig. 4) (a) and the dependence of the THz pulse generation efficiency F on the laser beam radius r calculated from the data of Fig. 4 (b).

theoretical dependence substantially differs from the experimental one. Therefore, the decrease in the THz pulse generation efficiency with increasing laser radiation intensity and simultaneous decreasing the laser beam diameter cannot be explained by the influence of TPA only. We assume that the attenuation of THz radiation is mainly determined by the laser beam diameter (Fig. 6b).

3.2 Role of fundamental radiation focusing

THz pulses are usually recorded with a photoconductive antenna or an electro-optic detector. Both these methods measure the electric field strength E_{ter}, while all optical detectors and a bolometer measure the intensity proportional to E_{ter}^2 (or power). This essentially changes the role of laser radiation focusing during optimisation of the THz pulse intensity. Nevertheless, the z-hole was observed both upon measuring the THz field with a dipole antenna and upon measuring the THz pulse power with a bolometer (Fig. 7a).

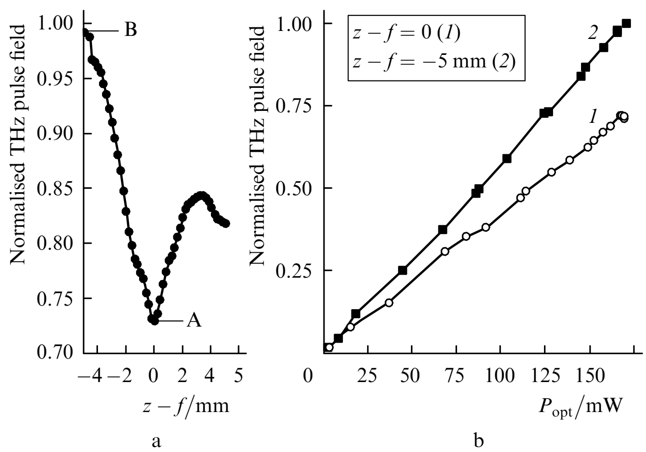

Figure 7. Dependence of the THz pulse field on the distance $z - f$ obtained by the z-scan method and measured with an antenna ($d = 2$ mm, $f = 50$ mm) (a) and the dependence of the THz pulse field on the laser radiation power for points A (1) and B (2) shown in Fig. 7a for $d = 2$ mm and $f = 50$ mm (b).

In the case of nonlinear (quadratic) optical processes, the measured power P_{sig} of a nonlinear signal can be considerably increased by focusing fundamental radiation. This can be achieved because $I_{\mathrm{sig}} \propto (\chi^{(2)} E_{\mathrm{opt}}^2)^2$, $E_{\mathrm{opt}} \propto (P_{\mathrm{opt}}/S)^{1/2}$, and $P_{\mathrm{sig}} \propto I_{\mathrm{sig}} S \propto P_{\mathrm{opt}}^2/S$, where P_{opt} is the fundamental radiation power and S is the laser spot area on a sample. Upon focusing the value of S is reduced by two-three orders of magnitude at the constant power P_{opt}, and since $P_{\mathrm{sig}} \propto P_{\mathrm{opt}}^2/S$, the corresponding increase in the nonlinear signal P_{sig} is observed.

In the case of THz pulse generation with the help of optical rectification ($E_{\mathrm{ter}} \propto P_{\mathrm{opt}}/S$) and detection of the THz pulse field E_{sig} with a dipole antenna, a tighter focusing of laser radiation into a crystal generating THz pulses should not enhance the measured signal. The dipole antenna measures the field E_{ter} rather than its square E_{ter}^2, so that $E_{\mathrm{sig}} \propto E_{\mathrm{ter}} S_{\mathrm{opt}}$. The increase in the intensity I_{opt} is compensated by the decrease in the beam spot area S, and the measured THz field strength is proportional only to the power P_{opt} of incident laser radiation and should not depend on focusing (on the area S). Only when the detector aperture is small compared to the beam spot area upon measuring the local field strength, laser radiation focusing can lead to a weak increase in the measured signal.

To separate the influence of the laser beam diameter on the THz pulse generation efficiency from the influence of nonlinear absorption, we measured the power dependences of the THz pulse generation efficiency for a constant beam diameter (Fig. 7b). The 770-nm, 170-mW laser radiation was focused by a lens with the focal distance $f = 50$ mm into a ZnTe crystal, and the dependence of the maximum amplitude of the THz pulse field on the laser beam power was measured. We performed two measurements: for $z = z_d$ ('z-hole') (point A in Fig. 7a), when the minimum THz pulse generation efficiency was observed ($z - f = 0$, the waist diameter is 24 μm, $I_{max} = 5$ GW cm^{-2}), and for the high THz pulse generation efficiency ($z - f = -5$ mm, the waist diameter is 200 μm, $I_{max} = 0.03$ GW cm^{-2}) (point B in Fig. 7a) outside the 'z-hole'. We measured the field (not power) of THz radiation integrated over the detector area as a function of the incident laser radiation power P_{opt}. The strength of the THz field linearly depends on the power P_{opt} ($E_{ter} \propto E_{opt}^2 \propto P_{opt}$) if the role on nonlinear absorption is small. Both these power dependences proved to be linear (Fig. 7b) (the effect of TPA is small even when the crystal is located in the beam waist).

If the THz 'z-hole' was caused by the influence of nonlinear processes, then experimental curve (*1*) in Fig. 7b in the region of high powers would saturate or even decrease. The saturation of the dependence $E_{ter}(I_{opt})$ would result in the smoothing of the maximum of the dependence $P_{ter}(z-f)$ (Fig. 6a), while the local minima of the dependences $P_{ter}(z-f)$ (Fig. 6a) and $E_{ter}(z-f)$ (Fig. 7a) can be observed, according to our assumption, only when $E_{ter}(I_{opt})$ decreases at high powers. Because our experimental data show neither the saturation nor decrease of $E_{ter}(P_{opt})$ for $z = z_d$ [curve (*1*) in Fig. 7b], we conclude that the THz 'z-hole' is not related to nonlinear-optical processes.

3.3 Role of a THz source size

Consider the role of the transverse size of a laser beam (source size and the THz pulse generation region). This size should affect the THz beam divergence and can also affect the THz pulse generation efficiency. We determined the divergence of THz radiation by measuring the radiation patterns near the crystal (at a distance of 32 mm) and far from it (at a distance of 300 mm).

At small distances from the crystal, the THz radiation pattern was measured using an aperture with a variable radius r_d (Fig. 8a). Only the central part of the THz beam ($r < r_d$) was incident on the antenna detector. By assuming that the transverse field distribution is Gaussian and placing the aperture centre on the THz beam axis, we can estimate the beam radius on the aperture and the radiation divergence from the dependence of the amplitude of the transmitted THz pulse on the aperture radius. The dependence of the field amplitude E_{ter} on r_d should have the form $E_{ter}(r_d) \propto E_{max}\{1 - \exp[-(r_d/r_0)^2]\}$, by neglecting diffraction from the aperture.

Let us compare the angular divergence of radiation for two positions of a focusing lens corresponding to points A and B in Fig. 7a. The model curve for $z - f = 5$ mm is shown in Fig. 8a. By comparing the model and experimental data, we see that the THz beam radius is ~ 4.3 mm,

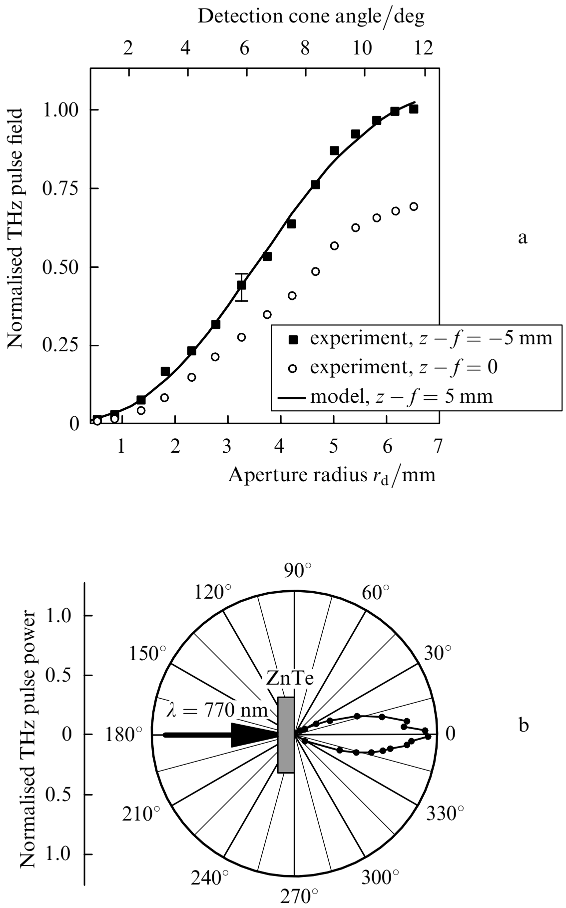

Figure 8. Dependences of the THz field amplitude on the aperture radius r_d measured with an antenna for two positions of a focusing lens, $f = 50$ mm and $d = 2$ mm when the aperture was located in the THz beam at a distance of 32 mm from the ZnTe crystal (a) and the THz radiation pattern for $z - f = 8$ mm, $f = 80$ mm, and $d = 2$ mm measured by a bolometer at a distance of 300 mm from the ZnTe crystal with the angular resolution of 2° (b).

corresponding to the angular divergence $\sim 7.6°$. When the optical beam was tightly focused into the crystal, i.e., when $z - f = 0$ (the amplitude of the transmitted THz field reduced by 40%), the beam radius was measured to be ~ 4.7 mm, while the angular divergence increased up to 8.3° (by 9 %). Therefore, the increase in the THz radiation divergence upon optical beam focusing is not the only reason for strong attenuation of the THz signal.

The THz radiation pattern was measured more accurately at a distance of 300 mm from the ZnTe crystal by using a bolometer, which was moved around the crystal (Fig. 8b). In this case ($z - f = 8$ mm, $f = 80$ mm), the angular divergence of the THz radiation was 15°.

Note that upon focusing laser radiation into the crystal, the size of the THz pulse source becomes comparable with the wavelength of THz radiation, whose divergence should tend in this case to 4π. In our case, the THz pulse generation occurs over the entire crystal thickness ($d = 2$ mm). The group velocities of optical and THz pulses in a ZnTe crystal virtually coincide ($\Delta n \approx 0.09$) [13] (see Table 1), while the coherence length upon the THz pulse generation is ~ 3 mm. The THz radiation generated at each point z of the crystal (radiation from each point has a high divergence) interfere constructively only in the propagation direction of the optical pulse. This interference determines the resulting directivity of THz radiation generated in the ZnTe crystal. Therefore, the wave front of THz radiation at the crystal output is comparable, under our experimental conditions, with the wave front of the fundamental (focused) laser radiation. However, according to the diffraction law, during propagation in a free space the THz beam diverges stronger than the optical beam because $\lambda_{ter} \gg \lambda_{opt}$. The diffraction-limited divergence of the THz beam is one of the factors restricting the expediency of fundamental beam focusing.

3.4 Dependence of the THz pulse power on the beam radius

We assume that when the transverse size of a THz source (the waist diameter 20 – 100 μm) becomes smaller than the radiation wavelength $\lambda_{ter} = 300$ μm, the THz pulse generation efficiency decreases with decreasing the source size due to diffraction. Such a decrease in the THz pulse generation efficiency was experimentally observed in [25] and described by the known Bethe theory [26] for diffraction of waves propagating through an aperture of diameter much smaller than the wavelength.

Let us construct an approximate (neglecting divergence and dispersion) phenomenological model describing the dependence of the THz power on a laser beam diameter. Consider the function $P_{ter}(I_{opt}, r) \sim g(I_{opt})F(r)$, where $g(I_{opt})$ is the laser radiation intensity distribution in a crystal; $F(r)$ is the function determining the dependence of the THz pulse generation efficiency only on the beam radius in the crystal. The dependence $g(I_{opt})$ is described by expression (4) and takes into account a change in the laser radiation intensity caused by nonlinear absorption and focusing; the dependence $P_{ter}(I_{opt}, r)$ was measured experimentally. From these data, the required function $F(r)$ is determined. Figure 6b shows the function $F(r)$ obtained from the data presented in Fig. 4. One can see that, within the framework of our model, as the laser beam radius inside the ZnTe decreases, the power of THz pulses also decreases with respect to their power that could be obtained at laser radiation intensities used in experiments.

Another factor affecting the intensity of the THz signal is the detector aperture. We used in our experiments a detecting antenna with the effective input aperture of radius $r_a \approx 2$ mm. If the optical beam radius r_{opt} and correspondingly the THz beam radius inside the ZnTe crystal exceeds this radius ($r_{opt} > r_a$), then not the entire THz field is involved in the generation of the signal detected. Therefore, to detect the maximum THz signal, the optical beam radius inside the crystal should be smaller than the effective aperture of the antenna but larger than the THz wavelength: $r_a \gg r_{opt} \gg \lambda_{ter}$. By moving the focusing lens along the z axis, it is convenient to optimise the laser beam radius inside the crystal, thereby obtaining the maximum THz signal.

4. Conclusions

We have studied the generation of THz pulses in a nonlinear-optical ZnTe crystal due to optical rectification. A substantial decrease in the THz pulse power was observed upon tight focusing femtosecond pulses into the crystal. It has been shown that for the optimal use of the ZnTe crystal for generating THz pulses, the following circumstances should be taken into account:

(i) Focusing laser radiation into a nonlinear crystal is justified only when the beam waist radius exceeds the THz pulse wavelength, which is approximately 300 μm. In the case of a tighter focusing, the THz pulse power substantially decreases. The maximum THz pulse generation efficiency is achieved when the distance z from the lens to the crystal is smaller than the focal distance f. Focusing laser radiation on the THz pulse generator is undoubtedly justified in three cases: when the THz pulse field power is measured rather than its strength, when the detector aperture is small, and when the THz pulse generator is small.

(ii) The decrease in the THz radiation power upon tight focusing of a laser beam into a crystal is not caused by nonlinear absorption or any other processes whose efficiency is proportional to the optical radiation intensity. TPA and SHG accompanying the THz pulse generation do not play a substantial role when the peak intensity of fundamental radiation is lower than 3 – 5 GW cm^{-2}. However, based on the TPA coefficient measured in our study ($\beta = 20 \pm 5$ cm GW^{-1}), we can assume that at high peak intensities of fundamental radiation TPA can limit the THz pulse generation efficiency and even lead to the optical breakdown in the crystal.

Acknowledgements. The authors thank V.V. Kocharovskii and V.V. Shuvalov for useful discussions of the results and A.V. Balakin for his help in experiments. This work was partially supported by the Russian Foundation for Basic Research (Grant Nos 04-02-17354-a and 04002-16866) and the Scientific Program 'Universities of Russia'.

References

1. Leitenstorfer A., Hunsche S., Shah J., Nuss M.C., Knox W.H. *Appl. Phys. Lett.*, **74**, 1516 (1999).
2. Xu L., Zhang X.-C., Auston D. *Appl. Phys. Lett.*, **61**, 1784 (1992).
3. Ferguson B., Wang S., Gray D., Abbot D., Zhang X.-C. *Opt. Lett.*, **27**, 1312 (2002).
4. Auston D.H., Cheung K.P., Valdmanis J.A., Kleinman D.A. *Phys. Rev. Lett.*, **53**, 1555 (1984).
5. Auston D.H. *Appl. Phys. Lett.*, **26**, 101 (1975).
6. Zhang X.-C., Auston D.H. *J. Electron. Wave Appl.*, **6**, 85 (1992).
7. Van Exter M., Grischkowsky D.R. *IEEE Transactions on Microwave Theory and Techniques*, **38**, 1684 (1990).
8. Grischkowsky D., in *Frontiers in Nonlinear Optics* Ed. by H. Walther, N. Koroteev, M.O. Scully (Philadelphia, Institute of Physics, 1993) p. 196.
9. Abdulin U.A., Lyakhov G.A., Rudenko O.V., Chirkin A.S. *Zh. Eksp. Teor. Fiz.*, **66**, 1295 (1974).
10. Aristov V.V., Tsyrul'nikov D.A. *Kvantovaya Elektron.*, **25**, 1118 (1998) [*Quantum. Electron.*, **28**, 1082 (1998)].
11. Ding Y., Zotova I. *Opt. Quantum Electron.*, **32**, 531 (2000).
12. Cote D., Sipe J.I., Driel H.M. *J. Opt. Soc. Am. B*, **20**, 1374 (2003).
13. Nahata A., Weiling A.S., Heintz T.F. *Appl. Phys. Lett.*, **69**, 2321 (1996).
14. Nazarov M.M., Sapozhnikov D.A., Shkelnyuk S.A., Shuvaev A.V., Shkurinov A.P. *Proc. Joint XXIX Int. Conf. on Infrared and Millimeter Waves and XII Int. Conf. on Terahertz Electronics* (University of Karlsruhe, Germany, 2004) p. 359.
15. Duvillaret L., Garet F., Coutaz J.-L. *IEEE J. Sel. Top. Quantum Electron.*, **2**, 739 (1996).
16. Schall M., Jepsen P.U. *Appl. Phys. Lett.*, **80**, 4771 (2002).
17. Grigor'ev I.S., Meilikhov E.Z. (Eds) *Fizicheskie velichiny. Spravochnik* (Handbook of Physical Quantities) (Moscow: Energoatomizdat, 1991) pp 864, 883, 893.
18. Bechtel J.H., Smith W.L. *Phys. Rev. B*, **13**, 3515 (1976).

19. Yin M., Li H.P., Tang S.H., Ji W. *Appl. Phys. B*, **70**, 587 (2000).
20. Gallot G., Zang J., McGowan R.W., Jeon T.I., Grishkovsky D. *Appl. Phys. Lett.*, **74**, 3450 (1999).
21. Kröll J., Darmo J., Unterrainer K. *Proc. Joint XXIX Int. Conf. on Infrared and Millimeter Waves and XII Int. Conf. on Terahertz Electronics* (University of Karlsruhe, Germany, 2004) p. 465.
22. Eriksson A., Lindgren M., Svensson S., Arntzen P.-O. *J. Opt. Soc. Am. B*, **15**, 810 (1998).
23. Tiedje H.F., Haugen H.K., Preston J.S. *Proc. Joint XXIX Int. Conf. on Infrared and Millimeter Waves and XII Int. Conf. on Terahertz Electronics* (University of Karlsruhe, Germany, 2004) p. 363.
24. Akhmanov S.A., Nikitin S.Yu. *Physical Optics* (Oxford: Clarendon Press, 1997; Moscow: Izd. Moscow State University, 1998).
25. Xu J.Z., Zang X.-C. *Opt. Lett.*, **27**, 1067 (2002).
26. Bethe H.A. *Phys. Rev.*, **66**, 163 (1944).